

# Mechanism of Ferroelectricity in $d^3$ Perovskites - a Model Study

Paolo Barone<sup>1</sup>, Sudipta Kanungo<sup>2</sup>, Silvia Picozzi<sup>1</sup>, and Tanusri Saha-Dasgupta<sup>2</sup>

1. CNR-SPIN 67100 L'Aquila, Italy and

2. S. N. Bose National Centre for Basic Sciences,  
Sector III, Block JD, Salt Lake, Kolkata 700 098, India

By means of a model Hamiltonian approach we study the role of volume expansion, Hund's coupling and electron correlation in the standard hybridization mechanism for ferroelectricity in cubic  $\text{CaMnO}_3$ , a prototypical non- $d^0$  perovskite. Our results establish that the ferroelectric instability arises from a subtle balance between different energy contributions, explaining the origin of its enhancement under negative pressure. Expansion of volume is found to cause a strong reduction of the elastic energy, while leaving almost unchanged the tendency of Mn states to form covalent bonds with the surrounding oxygens. Hund's coupling with local spins of magnetic cations can reduce and even suppress the instability towards the ferroelectric state.

PACS numbers: 71.10.Fd, 75.47.Lx, 77.80.-e, 71.15.-m

## I. INTRODUCTION

Since the revival of interest in the magnetoelectric effect due to the possibility of multiferrocity<sup>1</sup> with simultaneous presence of ferroelectric and magnetic order, many attempts have been made to create multiferroic materials focusing on the wide variety of transition metal  $\text{ABO}_3$  perovskites.

The classical ferroelectrics as well as many magnetic materials belong<sup>2,3</sup> to this class of compounds. However, overlap between ferroelectric perovskites and magnetic perovskites are rare, with the exception of compounds like  $\text{BiFeO}_3$  and  $\text{BiMnO}_3$ . This lead to the suggestion of general "exclusion" rule for perovskites<sup>4-7</sup>, according to which ferroelectricity occurs for  $d^0$  B site transition-metal ( $TM$ ) cation<sup>8</sup>, while the magnetism requires  $d^n$  B site cations with  $n \neq 0$ . This mutual exclusion of ferroelectric and magnetic properties is rationalized by the cases of conventional ferroelectric perovskites like, e.g.,  $\text{BaTiO}_3$ ,  $\text{KNbO}_3$  or  $\text{Pb}(\text{ZrTi})\text{O}_3$ , for which the driving force behind the ferroelectric distortion comes from the tendency of  $TM$  empty  $d$  states to establish a strong covalency with the surrounding oxygens.<sup>6,9</sup> The hybridization driven mechanism is maximally efficient when the antibonding states, with predominant  $TM$   $d$  character, are completely empty, hence for  $d^0$  B site perovskites. The above mentioned exclusion principle is violated for cases like  $\text{BiFeO}_3$  and  $\text{BiMnO}_3$ , for which the polarization arises in A sublattice due to the lone-pair stereochemical activity of Bi 6s electrons<sup>10</sup> and magnetism arises in B sublattice, with no apparent coupling between the two order parameters. For technological purpose, on the other hand, it is highly desirable to invoke coupling between the two order parameters, so that magnetism can be controlled by electric field and polarization by magnetic field. Along this line of thought, a number of magnetically induced multiferroic perovskites have been synthesized and studied, in which the complicated magnetic structure either with non-collinear spiral spin configuration<sup>11-13</sup> or collinear  $\uparrow\uparrow\downarrow\downarrow$  E-type antiferromagnetic<sup>14-16</sup> structure, breaks the inversion symmetry and induces polarization.

Also non-trivial charge distributions in systems displaying both charge and/or orbital order may significantly contribute to the onset of polar ferroelectric phases<sup>17-19</sup>, even concomitantly with magnetism. These compounds, known as improper ferroics, normally do not exhibit off centric movement of magnetic cations. While such electronically driven mechanism has generated lot of academic interest, the resulting polarization is often tiny, precluding technological applications. Search is, therefore, on to obtain multiferroic materials showing magnetoelectric coupling with reasonably high transition temperature and polarization values.

Since the conventional lattice driven mechanism of polarization with off centric movement of B site cations arises due to delicate balance between the hybridization energy gain and the repulsive electrostatic energy, the general applicability of the "exclusion principle" for a  $d^n$  perovskite with  $n < 5$  is difficult to predict a-priori.  $d^n$  perovskite, if can be made to a conventional ferroelectric, is expected to exhibit magnetoelectric coupling as well as presumably large values of polarization. Mn based perovskites like  $\text{CaMnO}_3$ ,  $\text{BaMnO}_3$  or  $\text{SrMnO}_3$  may be considered as possible candidates, since B site cation in this case is in a  $d^3$  electronic configuration, with electrons occupying, within a cubic crystal field, the 3-fold degenerate  $t_{2g}$  states, leaving the  $e_g$  states unoccupied. Noticeably, like conventional  $d^0$  ferroelectric perovskites, they exhibit anomalously large Born effective charges (BECs) of Mn ions.<sup>20-22</sup> The study by Ederer *et al.*<sup>20</sup> showed that the largest anomalous contributions to BECs can be understood in terms of a charge transfer between  $TM$   $d$  and O  $p$  states along the  $\sigma$ -type channel, suggesting that the hybridization mechanism is mostly  $e_g$ -driven. Attempts have been made to induce ferroelectricity in these compounds through increase of volume by applying negative or chemical pressure<sup>21,22</sup>, or in epitaxially strained thin films<sup>23</sup>. Interestingly, the polarization in these predicted systems may be larger than that typically expected in magnetically-induced multiferroics such as  $\text{TbMnO}_3$  ( $P \lesssim 0.1 \mu\text{C}/\text{cm}^2$ ) or  $\text{HoMnO}_3$  ( $P \sim 0.5 - 2 \mu\text{C}/\text{cm}^2$ ). Rather large polarization value

of  $P = 54 \text{ } \mu\text{C}/\text{cm}^2$  has been predicted for epitaxially strained  $\text{SrMnO}_3$ .<sup>23</sup>

A microscopic understanding of this interesting behavior demands further study, in particular what makes ferroelectric instability stronger at larger lattice constants. Hybridization effect is expected to be weaker for increased  $TM$  - O bondlengths and therefore would disfavor the hybridization-driven ferroelectricity even further. The role of Hund's coupling between  $t_{2g}$  and  $e_g$  spins, which has been suggested<sup>6</sup> to prevent ferroelectricity in compounds like  $\text{CaMnO}_3$ , needs to be also understood in the context of increased lattice constant. In the present study, we investigated this issue in a model Hamiltonian based approach. The model Hamiltonian approach, as opposed to the first-principles density functional theory (DFT) calculations, has the advantage of analysing the different energy contributions individually and providing a microscopic understanding of the influence of various different factors. However, since the ferroelectric instability arises due to delicate balance between different competing energies, we employ DFT tools for accurate estimates of different energies. Specifically, we have used muffin-tin orbital (MTO) based NMTO-downfolding technique<sup>24</sup> to estimate the hopping interactions between nearest neighbor Mn and oxygen atoms, and that between next nearest neighbor oxygens. The energy associated with the stiffness of the off-centric, ferroelectric movement has been estimated using total-energy DFT calculations carried out employing the plane-wave pseudopotential method as implemented within VASP.<sup>25</sup> We assumed the high temperature cubic crystal structure of  $\text{CaMnO}_3$ , which is the prototypical cubic  $TM$  perovskite crystal structure. We have not considered in our study the antiferrodistortive tilt and rotation of  $\text{MnO}_6$  octahedra which have been found<sup>21,22</sup> to compete with the ferroelectric instability. Our study, therefore, focuses on the competition between the pair-breaking Hund's rule coupling, the hybridization effect and the short-range, electrostatic repulsion in destabilizing or stabilizing ferroelectricity in a prototypical cubic perovskite structure, and the effect of volume expansion on it.

## II. METHODS AND COMPUTATIONAL DETAILS

For our study, we used a minimal model designed to reproduce the tendency of empty  $e_g$  states to establish covalent bonds with surrounding oxygens. Neglecting the  $t_{2g}$  electrons motion, the model should describe the hopping between filled oxygen  $p$  state and empty Mn two-fold  $e_g$  states on the background of localized  $t_{2g}$  spins. Within the cubic crystal field, the  $e_g$  states establish prevalently  $\sigma$  bonds with O  $p$  states parallel to the bond direction<sup>26</sup>, as confirmed by Wannier function analysis<sup>20,27</sup>. We therefore considered a 5-band  $d - p$

model, given by  $H = H_d + H_p + H_{dp}$ , where

$$H_d = \varepsilon^d \sum_{i,\alpha,\sigma} d_{i\alpha\sigma}^\dagger d_{i\alpha\sigma} - J_H \sum_i \mathbf{s}_i \cdot \mathbf{S}_i + H_{e-e} \quad (1)$$

takes into account the local physics on  $TM$  site,

$$H_p = \varepsilon_0^p \sum_{j,\sigma} p_{j\sigma}^\dagger p_{j\sigma} + \sum_{j,j',\sigma} t_{j,j'}^{pp} p_{j\sigma}^\dagger p_{j'\sigma} \quad (2)$$

describes the oxygen sites, and

$$H_{dp} = \sum_{i,j,\alpha,\sigma} V_{i,j}^\alpha d_{i\alpha\sigma}^\dagger p_{j\sigma} \quad (3)$$

describes the hybridization between Mn and O sites.  $d_{i,\alpha,\sigma}^\dagger$  creates an electron with spin  $\sigma$  on a Mn at site  $i$  and in the orbital state  $x^2 - y^2$  ( $3z^2 - r^2$ ) for  $\alpha = 1(2)$ , while  $p_{j,\sigma}^\dagger$  creates an electron on O site  $j = i \pm \hat{e}/2$ , with  $\hat{e}$  the direction unit vector  $\hat{x}, \hat{y}, \hat{z}$ , in the orbital state  $x, y, z$  respectively.  $\varepsilon_0^{d(p)}$  is the  $d(p)$  onsite energy of Mn  $e_g$  (O- $p$ ), whereas  $t_{j,j'}^{pp}$  and  $V_{i,j}^\alpha$  are hopping parameters that describe hybridization between neighboring O  $p$  states and between Mn  $e_g$  states and O  $p$  states, respectively.

In order to get a faithful estimate of the onsite energies and the hopping interactions, we have carried out NMTO-downfolding calculations<sup>24</sup>. Starting from a full DFT calculation for cubic  $\text{CaMnO}_3$ , NMTO-downfolding arrives at a 5-orbital Hamiltonian by integrating out degrees of freedom involving Mn- $t_{2g}$ , O- $p_\pi$  and those involving Ca. The downfolded 5-orbital Hamiltonian is built by defining energy-selected, effective Mn- $e_g$  and O- $p_\sigma$  orbitals which serve as Wannier-like orbitals spanning the downfolded five bands. Linear muffin-tin calculations (LMTO)<sup>28</sup> were performed in order to evaluate self-consistently the potential parameters needed for the NMTO procedure.

The second and third term in Eqn. (1) describe the Coulomb interactions in the  $3d$  shell of the  $TM$  cation. Treating the  $t_{2g}$  electrons as classical spins  $\mathbf{S}_i$ , the interaction between them and the  $e_g$  electrons can be accounted for by the Hund's coupling  $J_H$ , connecting the localized core spins  $\mathbf{S}_i$  with the spins  $\mathbf{s}_i = \sum_{\alpha,\sigma,\sigma'} d_{i\alpha\sigma}^\dagger \hat{\tau}_{\sigma\sigma'} d_{i\alpha\sigma'}$  of the mobile electrons,  $\hat{\tau}$  being the Pauli matrices, as given in the second term in Eqn. (1). In most of our calculations, we have assumed the antiferromagnetic G-type arrangement of  $t_{2g}$  spins, though to study the influence of spin arrangements, we have also considered the ferromagnetic alignment of  $t_{2g}$  spins. The third term,  $H_{e-e}$  describes the Coulomb interactions between  $e_g$  electrons, as given below. We drop the site

index for sake of simplicity.

$$\begin{aligned}
H_{e-e} = & \frac{U}{2} \sum_{\alpha,\sigma} n_{\alpha\sigma} n_{\alpha\bar{\sigma}} + \\
& \frac{U'}{2} \sum_{\alpha,\alpha',\sigma,\sigma'} (1 - \delta_{\alpha\alpha'}) n_{\alpha\sigma} n_{\alpha'\sigma'} + \\
& \frac{J}{2} \sum_{\alpha,\alpha',\sigma,\sigma'} \left[ (1 - \delta_{\alpha\alpha'}) d_{\alpha\sigma}^\dagger d_{\alpha'\sigma'}^\dagger d_{\alpha\sigma} d_{\alpha'\sigma'} + \right. \\
& \left. (1 - \delta_{\alpha\alpha'}) (1 - \delta_{\sigma\sigma'}) d_{\alpha\sigma}^\dagger d_{\alpha'\sigma'}^\dagger d_{\alpha'\sigma'} d_{\alpha\sigma} \right],
\end{aligned} \tag{4}$$

$U, U', J$  are the intraband Coulomb, interband Coulomb and interband exchange couplings respectively<sup>29</sup>, defined within the  $e_g$  manifold. The values of  $U, U', J$  were estimated as,  $U = 7.02$  eV,  $U' = 4.97$  eV and  $J = 1.025$  eV, as relevant for  $\text{CaMnO}_3$ .<sup>30</sup> Treating  $H_{e-e}$  at the mean-field level, applying a standard Hartree-Fock linearization of two-body operators, the problem reduces to a single-particle problem, which can be solved straightforwardly in reciprocal space. Considering the fact that the  $e_g$  manifold is empty, such a mean-field treatment is justified. In order to take into account the G-type antiferromagnetic configuration of  $t_{2g}$  spins, we defined a unit cell hosting two  $TM$  cations and six O ions<sup>31</sup>. After transformation in reciprocal space, the Hamiltonian can be diagonalized for any given value of momentum  $k$ ; integration was then performed using a nested Clenshaw-Curtis quadrature rule<sup>32</sup>.

In order to investigate the ferroelectric instability, we considered an off-centering displacement  $u$  of each Mn cation along the  $+\hat{z}$  direction, *i.e.*, towards one of the apical oxygen, as considered in Ref. 20. The corresponding hopping parameters were modified proportionally to  $\sim (d/d_0)^{-3.5}$ ,  $d$  and  $d_0$  being the distorted and undistorted Mn-O bond lengths<sup>33</sup> respectively.<sup>34</sup> The elastic energy loss associated with the distortion,  $u$ , was evaluated using total-energy DFT calculations, as mentioned earlier. The plane wave calculations, carried out for this purpose, were performed using projector augmented wave (PAW) potentials<sup>35</sup> and the wavefunctions were expanded in the plane wave basis with a kinetic energy cut-off of 450 eV. Reciprocal space integration was carried out with a  $k$ -space mesh of  $6 \times 6 \times 6$ .

### III. RESULTS

#### A. Volume effects on covalency energy, role of correlation and Hund's coupling

Using the NMTO-downfolding technique, as explained in Section II, we evaluated the onsite energies and various hopping interactions, relevant for  $\text{CaMnO}_3$  for two cubic crystal structures, one at equilibrium volume<sup>36</sup> with lattice constant  $a_0 = 3.73$  Å and another at increased volume, as under a negative isotropic pressure, with 2%

increased lattice constant  $a_0 = 3.805$  Å. The obtained parameters are listed in Table I. The hopping interactions between Mn and O sites is given by,  $V_{ij}^\alpha = (-1)^{M_{ij}} t_{pd}^{\alpha\beta}$ , where  $M_{ij} = 2$  if  $j = i + \hat{e}/2$  and  $M_{ij} = 1$  if  $j = i - \hat{e}/2$ ;  $\beta = x, y, z$  labels the  $p$  orbital state that hybridize with Mn  $e_g$  states. Within a cubic symmetry, the interaction between  $TM$   $x^2 - y^2$  and O  $p_z$  is zero, and therefore not listed in the table.

	$\varepsilon_d$	$\varepsilon_p$	$t_{pd}^{1,z}$	$t_{pd}^{1,x(y)}$	$t_{pd}^{2,x(y)}$	$t_{pp}$
eq	-2.86	-5.16	1.95	1.69	0.98	0.75
2%	-3.10	-5.03	1.76	1.53	0.88	0.59

TABLE I: Onsite and hopping parameters at equilibrium and 2% increased lattice constant, obtained from NMTO-downfolding calculations.

Naively, one would expect that the tendency to form strong covalent bonds would decrease in the expanded volume structure. As is seen from the parameters listed in Table I, the hopping parameters are reduced by  $\sim 10\%$  upon 2% increase in lattice constant. However, interestingly, the volume expansion also influences the level splitting between  $d$  and  $p$  states, as is seen in Table I. Following Khomskii<sup>6</sup>, one can estimate the energy gain due to the off-centering of the  $TM$  ion, as described below. When a Mn atom shifts towards an apical oxygen, reducing the corresponding Mn-O bond length, it forms a strong covalent bond with this particular oxygen at the expense of weakening the bonds with other oxygen ions. Within a linear approximation and neglecting the bonds between the Mn ion and the in-plane oxygens, whose bond lengths are only slightly increased in the considered off-center shift, the covalency energy gain can be estimated as  $\delta E_{cov} \approx -2(u t_{pd})^2 / \Delta$ ,  $\Delta$  being the charge-transfer energy, given by  $|\varepsilon_d - \varepsilon_p|$ . An estimate of the changes in covalency energy gain induced by volume expansion may be obtained by considering the ratio  $t_{pd}^2 / \Delta$ , rather than hopping parameters  $t_{pd}$  only. As given in Table I, upon volume expansion  $\Delta$  is reduced by  $\sim 16\%$ , giving rise to a compensating effect of the reduction in hopping interaction. This leads to only a reduction by less than 4% in covalency energy gain upon volume expansion.

This above expectation is confirmed by our calculations on the model Hamiltonian. We carried out two sets of calculation, one excluding  $H_{e-e}$  and another including  $H_{e-e}$ . In both set of calculations, we assumed  $J_H = 0$ , therefore Hund's coupling was not operative. The results are shown in Fig. 1. As discussed in the above, the volume expansion was found to reduce the covalency energy gain due to off-centric movement marginally. Inclusion of correlation effects between  $e_g$  electrons, keeping  $J_H = 0$ , lead to a further suppression of the volume effect. This presumably is rationalized by the fact that inclusion of Coulomb interactions would tend to suppress hybridization interaction between oxygens and  $TM$  states, thus also making the effect of volume variation on hybridization energy gain less effective.

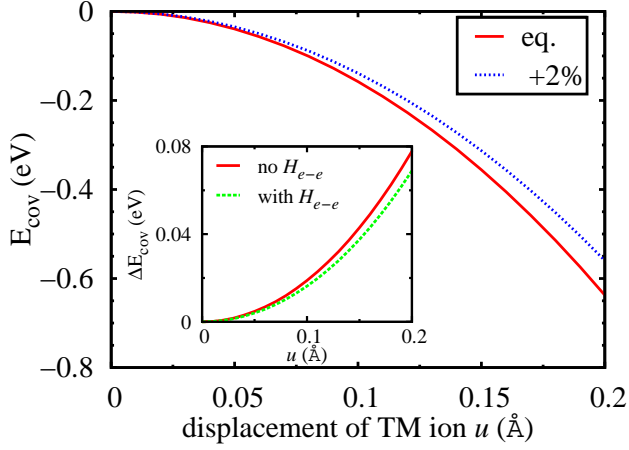


FIG. 1: Covalency energy in the 5-band model as a function of off-centering shift of Mn cation towards the apical oxygen at equilibrium and 2% increased lattice parameters, for  $H_{e-e}$  set to zero. Energies are shifted in such a way that  $E_{cov} = 0$  at  $u = 0$ . The negative values indicate a gain in covalency energy upon off centric movement. The inset shows the difference  $E_{cov}(2\%) - E_{cov}(eq.)$  with and without  $H_{e-e}$  but neglecting Hund's coupling.

In the next step, we investigated the role of Hund's coupling between mobile electrons and the localized spins on Mn ions. For this purpose, we evaluated the energy gain induced by the off-centering distortions at selected values of  $J_H$ , thus emphasizing its effect on the hybridization mechanism. We assumed G-type antiferromagnetic ordering for  $t_{2g}$  spins, which is the magnetic ordering observed for  $\text{CaMnO}_3$ . A realistic value for the Hund's coupling in manganites should be<sup>30,37</sup> between 1 and 2 eV. We have varied the  $J_H$  value from 0.5 to 2 eV. As proposed by Khomskii<sup>6</sup>, we find that the presence of local spins on the  $TM$  ions and their coupling to the mobile electrons through Hund's interaction reduces the energy gain due to the off centering movement. As discussed in Ref.6, the strong covalent bond between  $TM$   $e_g$  states and neighboring oxygen  $p$  states implies the formation of a singlet state. This is disfavoured by the strong Hund's coupling with the localized  $t_{2g}$  electrons on  $TM$  ion; this interaction can be seen as a local Zeeman field due to core spins and effectively acts as a “pair-breaker” on the singlet state<sup>6</sup>. This is demonstrated in the left panel of Fig. 2, where we plot the energy difference  $\Delta E_{cov} = [E_{cov}(u; J_H) - E_{cov}(u; J_H = 0)]$  as a function of the off-centering distortion  $u$ . We find this energy difference to be positive, indicating that introduction of  $J_H$  reduces the energy gain due to the off-centering movement. Increasing  $J_H$  reduces more and more the covalency energy, making  $\Delta E_{cov}$  more positive. Inclusion of electron-electron correlation within  $e_g$  manifold, through inclusion of  $H_{e-e}$  term, reduces the overall covalency energy due to off centering movement, as discussed in the context of Fig. 1. However, the relative energy loss in covalency energy due to the coupling with the underlying lo-

cal spins, expressed as  $E_{cov}(u; J_H = 2)/E_{cov}(u; J_H = 0)$ , remains similar between calculations excluding and including  $H_{e-e}$  term, as shown in the inset of left panel of Fig. 2. The calculations repeated for the 2% expanded lattice constant, exhibit the same trend, as shown in the right panel of Fig. 2. This leads us to conclude that the effectiveness or role of Hund's coupling to be nearly same for the equilibrium and the expanded volume.

The effectiveness of Hund's coupling, on the other hand, is found to depend strongly on the magnetic arrangements of the underlying  $t_{2g}$  spins. The above discussed set of calculations have been repeated for the ferromagnetic alignment of the  $t_{2g}$  spins. The results are summarized in Fig. 3 for the equilibrium volume. Comparing the values of  $\Delta E_{cov}$ , we find them to be much smaller than those calculated for the G-type antiferromagnetic ordering of  $t_{2g}$  spins and shown in Fig. 2, suggesting that Hund's coupling is much less effective.  $\Delta E_{cov}$  is even found to attain small, negative values for  $J_H$  between 1 – 1.5 eV for moderate values of off centering movement. Inclusion of  $H_{e-e}$ , makes the effect of  $J_H$  even milder, with much smaller values of  $\Delta E_{cov}$ , as shown in the inset of Fig. 3. This finding is in accordance with the predicted jump in polarization of epitaxially strained  $\text{SrMnO}_3$ , when the system undergoes an antiferromagnetic-ferromagnetic phase transition<sup>23</sup>.

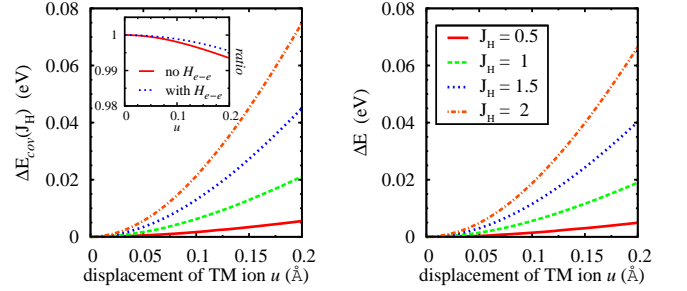


FIG. 2: Effect of Hund's coupling on the covalency energy at equilibrium (left) and expanded (right) volume as a function of the displacement  $u$  measured by the energy difference  $\Delta E_{cov}$ , neglecting other Coulomb interactions. The inset in the left panel shows the ratio  $E_{cov}(u; J_H = 2)/E_{cov}(u; J_H = 0)$ , measuring the relative energy loss with and without  $H_{e-e}$ .

## B. Estimation of elastic stiffness. Volume effect on total energy

The analysis, so far, has been restricted to the discussion of covalency energy gain due to off centering movement of  $TM$  cation. In order to arrive to a complete picture of polar instability, one needs to take into account the restoring force, which is given by the elastic stiffness associated to the displacement of  $TM$  cation. The elastic energy, that emerges from the short-range repulsive interactions between ions, for small displacements,



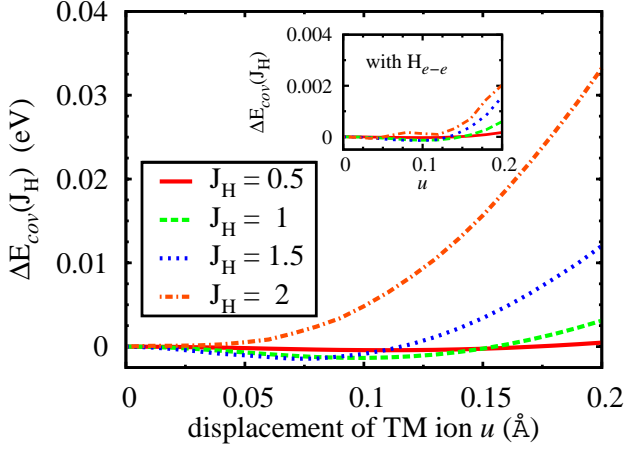


FIG. 3: Effect of Hund's coupling on the covalent energy gain at equilibrium volume as a function of the displacement  $u$  for a ferromagnetic ordering of local  $t_{2g}$  spins. The inset shows the same including  $H_{e-e}$ .

is expected to go as  $\sim k u^2/2$ ,  $k$  being the stiffness constant. We estimated the stiffness constant from total energy calculations carried out on plane wave basis. One may identify the covalency energy with the band energy contribution to the total energy, and the elastic energy as the remainder, *i.e.*  $E_{tot} = E_{cov} + E_{elas}$ . The relevant stiffness constant can then be extracted via a fitting procedure from the evolution of  $E_{elas}$  as a function of the shift  $u$ . This is shown in left panel of Fig. 4 for both the equilibrium and expanded volume. The fitting function was chosen as  $f(u) = k u^2/2 + c u^4$ . As shown in Table II, while the coefficient of the quartic term does not change in the expanded volume system with respect to the equilibrium case, the stiffness coefficient  $k$  is reduced by a factor of 0.4 in the expanded volume, suggesting a strong reduction of the repulsive short-range interactions.

	eq.	2%	eq.	2%
	$(E_{elas})$		$(F_{TM})$	
$k$ (eV/Å <sup>2</sup> )	12.365	4.961	10.846	4.291
$c$ (eV/Å <sup>4</sup> )	140	140	45	45

TABLE II: Stiffness constants as evaluated from estimates from elastic energies at equilibrium and 2% increased lattice parameters (shown in first and second columns respectively) and as evaluated from force acting on Mn cation (shown in third and fourth columns respectively).

In order to check the goodness of our estimate, we also adopted an alternative procedure of extracting the stiffness constant from the force acting on the *TM* ion. Right panel of Fig. 4 shows the evolution of the force acting on Mn ion,  $F_{Mn}$  as a function of the off centered displacement. The calculated data points were fitted with the function  $-f'(u) = -k u - 4c u^3$ . As shown in Table II, the estimated  $k$  coefficient shows same order of magnitude and same trend under volume expansion, whereas

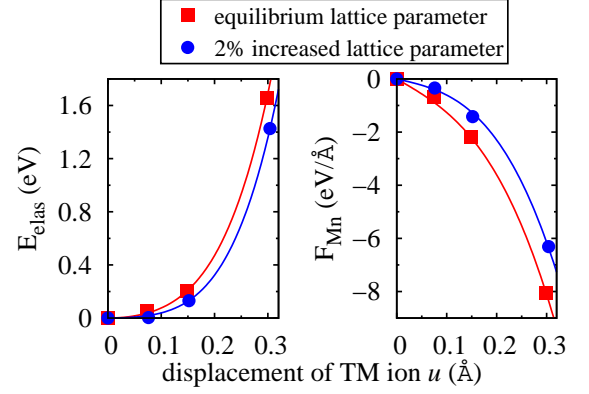


FIG. 4: The elastic energy (left panel) and force acting on Mn ion (right panel) plotted as a function of off centric displacement, obtained from DFT calculations.

the coefficient of the quartic term is more than three times smaller when evaluated from the total force. This finding, however, is not surprising if we notice that, in this second approach, we are neglecting forces acting on apical oxygens when we artificially shift the Mn cation. We, however, do not expect the physical picture to be change much between the two procedures, since in both the approaches, while the coefficient  $k$  was found to show a significant reduction under volume expansion, the coefficient of the quartic term,  $c$ , was found to remain unchanged by volume expansion.

From the knowledge of the stiffness constant and covalency energies, in the next step, we investigated the ferroelectric instability in cubic perovskite structure of  $\text{CaMnO}_3$  which arises due to the competition between the covalency energy and the elastic energy in the model Hamiltonian framework. With the estimated parameters discussed in previous sections, we find a weak ferroelectric instability for the system at equilibrium volume, which gets weakened more and more as we allow for a finite Hund's coupling between mobile electrons participating in the hybridization mechanism and the local Mn spins, finally nearly disappearing for  $J_H = 2$  eV, as shown in left top panel of Fig. 5. Upon increasing volume, however, a strong instability appears, which survives even after inclusion of Hund's coupling, though gets shifted to lower values of off centric displacement, as shown in left bottom panel of Fig. 5. In the above calculations,  $H_{e-e}$  was set to zero. Inclusion of  $H_{e-e}$ , as discussed in the above, weakens the covalency effect and the ferroelectric instability completely vanishes for the equilibrium volume, as shown in the right panels of Fig. 5. The ferroelectric instability, however, remains in the expanded volume, even for largest Hund's coupling strength of 2 eV.

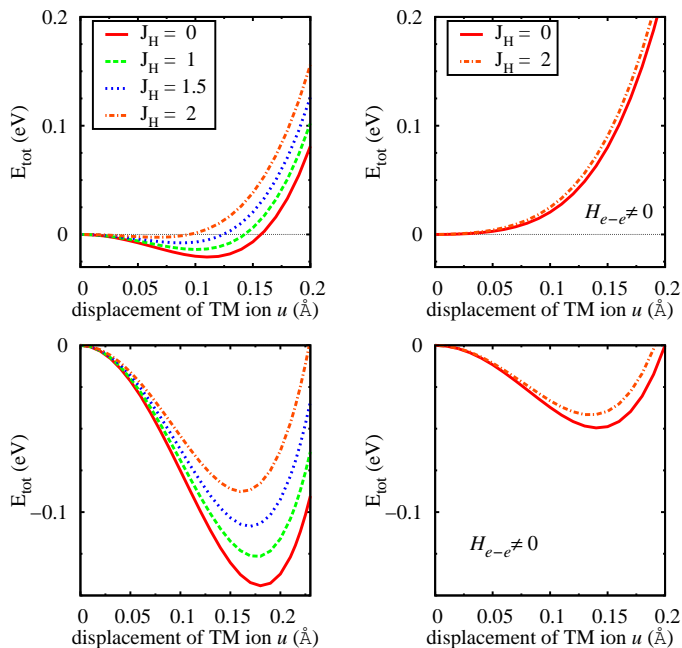


FIG. 5: Total energy calculated from the model Hamiltonian as a function of the off-centering shift of  $TM$  ion at equilibrium (top panels) and 2% increased lattice parameter (bottom panels) for different choice of Hund's coupling. Correlations within  $e_g$  electrons have been set to zero in left top and bottom panels, while they are included at the mean-field level in right top and bottom panels.

#### IV. CONCLUSIONS

To conclude, we have introduced a minimal 5-band  $d-p$  model with Coulomb interactions on the  $TM$  ion to describe the possible hybridization mechanism for ferroelectricity in magnetic Mn-based perovskites. As a case study, we have considered the cubic perovskite structure of  $\text{CaMnO}_3$  and have considered two different volumes of the structure, the equilibrium volume and 2% expanded volume. Our study shows that the ferroelectric instability crucially depends on the balance between two main energy contributions, one coming from the tendency of empty  $d$  states to form covalent bonds with surrounding O states and the other from the short-range forces between ions, resulting in an elastic energy associated to the  $TM$  off-centering shift. We found that volume expansion has marginal effect on the covalency energy gain, since the reduction in hopping interaction gets compensated by the simultaneous gain due to change in charge transfer energy. The coupling of the mobile electrons with localized spins on magnetic ions through Hund's interaction destabilizes the gain in covalency energy due to off centric movement, as has been suggested by Khomskii<sup>6</sup>. Interestingly, we find the influence of the Hund's coupling to crucially depend on the spin arrangements of the localized  $t_{2g}$  spins, suggesting a rather strong spin-phonon coupling, as predicted in epitaxially strained  $\text{SrMnO}_3$ <sup>23</sup>.

Since the hybridization driven mechanism turned out to be weakly volume dependent, the effectiveness of Hund's coupling in reducing the gain in covalency energy, which is a local effect, is found to be weakly affected by volume expansion. On the contrary, we found that the stiffness of the Mn off-centering displacement strongly depends on the volume, being more than halved for a 2% increase in lattice parameter. The strong reduction of short-range forces, combined with an almost unaffected tendency to covalency leads to stronger ferroelectric instability in expanded volume. The correlation between the  $e_g$  electrons has the role of suppressing the covalency effect, which washes out the weak ferroelectric instability found for the equilibrium volume, but retains the much more pronounced ferroelectric instability for the expanded volume.

Our results highlight the crucial role played by the balance of hopping integrals and charge-transfer energy in determining the effectiveness of the covalency. For instance, much weaker ferroelectric instability predicted for the iso-electronic  $d^3$   $\text{LaCrO}_3$  can be ascribed to a larger charge-transfer energy  $\Delta$ , as suggested in Ref. 20. On the other hand, one can speculate that the tendency to form covalent bonds is reduced for systems with partially filled  $t_{2g}$  states, e.g. with  $d^1$  or  $d^2$ , even if Hund's coupling is expected to play a less effective role compared to  $d^3$  configuration; in these systems, the empty  $t_{2g}$  electrons would establish  $\pi$  bonds with neighboring oxygens, implying smaller hopping integrals, whereas the charge-transfer energy is generally expected to be larger than that for  $d^3$  systems. The critical balance between different energy contributions needs to be estimated as in present case. It would, therefore, be interesting to repeat the above analysis for other  $d^n$  perovskite with  $n < 3$ .

Finally, it will be worthwhile to comment on the following. The ferroelectric instability in perovskite oxides is usually explained<sup>38</sup> in terms of a close competition between short-range (SR) forces, which tend to favor the non-polar cubic structure, and the long-range (LR) interactions, which tend to favor the ferroelectric phase. In particular, in Ref. 21 such SR and LR contributions have been discussed in the context of  $\text{CaMnO}_3$ . It may therefore be interesting to connect the various energy contributions discussed in the present work to SR and LR forces. Since the Hund's coupling as well as the restoring elastic stiffness tend to destabilize the ferroelectricity, they may be linked to SR forces. As detailed in Ref. 21, the LR contribution has been shown to be directly related to anomalously large Born effective charges (see also Ref. 39). We note that the presence of anomalously large charges originates from a change in the hybridization between occupied and unoccupied electronic states<sup>40</sup>. In the context of  $\text{CaMnO}_3$ , this translates to the change in hybridization or covalency between empty Mn  $e_g$  states and occupied O- $p$  states, which is in turn determined by both the hopping interaction,  $t_{pd}$ , and the charge transfer energy,  $\Delta$ , both affecting the LR forces.

*Acknowledgements* – We thank D. Khomskii for read-

ing the manuscript and for his helpful insights. This work has been supported by the European Community's Seventh Framework Programme FP7/2007-2013 under grant agreement No. 203523-BISMUTH. The project started during the AQUIFER research program held at CNR-

SPIN L'Aquila, Italy in September-October 2010 and sponsored by the NSF International Center for Materials Research at UCSB, USA. TSD would like to thank Advanced Materials Research Unit (AMRU) for financial assistance.

- 
- <sup>1</sup> M. Fiebig, J. Phys. D: Appl. Phys. **38**, R123 (2005)
  - <sup>2</sup> T. Mitsui *et al.*, Landolt-Börnstein, Numerical Data and Functional Relationships in Science and Technology, New Series Vol.16, 1, Springer, Berlin (1981).
  - <sup>3</sup> J.B. Goodenough and J.M. Longo, Landolt-Börnstein, Numerical Data and Functional Relationships in Science and Technology, New Series Vol.III.4, 126, Springer, Berlin (1970).
  - <sup>4</sup> N. A. Hill, J. Phys. Chem. B **104**, 6694 (2000).
  - <sup>5</sup> A. Filippetti and N. A. Hill, Phys. Rev. B **65**, 195120 (2002).
  - <sup>6</sup> D. I. Khomskii, J. Magn. Magn. Mater. **306**, 1 (2006).
  - <sup>7</sup> D. Khomskii, Physics **2**, 20 (2009).
  - <sup>8</sup> B. T. Matthias, Phys. Rev. **75**, 1771 (1949).
  - <sup>9</sup> R. E. Cohen, Nature **358**, 136 (1992).
  - <sup>10</sup> R. Seshadri and N. A. Hill, Chem. Mater. **13**, 2892 (2001).
  - <sup>11</sup> T. Kimura, T. Goto, H. Shintani, K. Ishizaka, T. Arima and Y. Tokura, Nature London **426**, 55 (2003).
  - <sup>12</sup> I. A. Sergienko and E. Dagotto, Phys. Rev. B **73**, 094434 (2006).
  - <sup>13</sup> H. Katsura, N. Nagaosa, and A. V. Balatsky, Phys. Rev. Lett. **95**, 057205 (2005).
  - <sup>14</sup> Y. J. Choi, H. T. Yi, S. Lee, Q. Huang, V. Kiryukhin, and S.-W. Cheong, Phys. Rev. Lett. **100**, 047601 (2008).
  - <sup>15</sup> I. A. Sergienko, C. Sen and E. Dagotto, Phys. Rev. Lett. **97**, 227204 (2006).
  - <sup>16</sup> S. Picozzi, K. Yamauchi, B. Sanyal, I. A. Sergienko and E. Dagotto, Phys. Rev. Lett. **99**, 227201 (2007).
  - <sup>17</sup> J. van den Brink and D.I. Khomskii, J. Phys.: Condens. Matter **20**, 434217 (2008).
  - <sup>18</sup> P. Barone, K. Yamauchi and S. Picozzi, Phys. Rev. Lett. **106**, 077201 (2011).
  - <sup>19</sup> P. Barone, S. Picozzi and J. van den Brink, Phys. Rev. B **83**, 233103(2011).
  - <sup>20</sup> C. Ederer, T. Harris, and R. Kováčik, Phys. Rev. B **83**, 054110 (2011).
  - <sup>21</sup> S. Bhattacharjee, E. Bousquet, and Ph. Ghosez, Phys. Rev. Lett. **102**, 117602 (2009).
  - <sup>22</sup> J. M. Rondinelli, A. S. Eidelson, and N. A. Spaldin, Phys. Rev. B **79**, 205119 (2009).
  - <sup>23</sup> J. H. Lee and K. M. Rabe, Phys. Rev. Lett. **104**, 207204 (2010).
  - <sup>24</sup> O. K. Andersen and T. Saha-Dasgupta, Phys. Rev. B **62**, R16219 (2000).
  - <sup>25</sup> G. Kresse and J. Furthmüller, Phys. Rev. B **54**, 11169 (1996).
  - <sup>26</sup> In the perfect cubic structure  $t_{2g}$  electrons hybridize mainly with O  $p - \pi$  orbitals, which do not hybridize with the  $e_g$ ; this independence of bonding mechanisms further supports our assumption of a 5-band model with localized  $t_{2g}$  spins.
  - <sup>27</sup> T. Saha-Dasgupta and S. Satpathy, J. Phys. (Condens. Matter) **15**, 1685 (2003).
  - <sup>28</sup> O. K. Andersen, Phys. Rev. B **12**, 3060 (1975).
  - <sup>29</sup> J. Kanamori, Prog. Theor. Phys. **30**, 275 (1963).
  - <sup>30</sup> J. van Elp and A. Tanaka, Phys. Rev. B **60**, 5331 (1999).
  - <sup>31</sup> In order to enforce the G-type antiferromagnetic configuration, we take advantage of the lattice being bipartite within cubic structure and assume staggered periodic boundary conditions, in such a way that a site belonging to sublattice A is connected only to sites belonging to sublattice B, both within the defined unit cell and through the boundaries.
  - <sup>32</sup> C. Clenshaw, A. Curtis, Numerische Mathematik, **2**, 197-205 (1960).
  - <sup>33</sup> W. A. Harrison, Electronic Structure and the Properties of Solids, Freeman, San Francisco, (1980).
  - <sup>34</sup> We considered only changes in  $\sigma$  bonding, neglecting possible small contributions from  $\pi$  bonding energies. Considering  $\pi$  bonding would imply extending the present 5-band model to an 11-band model taking into account all three  $p$  orbitals on each oxygen. We have checked the validity of our 5-band model results, in terms of comparison with calculations of 11-band model. We find the conclusions to remain unchanged with main changes to covalency energy coming from hybridization with apical oxygens, given by  $\sigma$  bonding.
  - <sup>35</sup> P. E. Blochl, Phys. Rev. B **50**, 17953 (1994). G. Kresse and D. Joubert, Phys. Rev. B **59**, 1758 (1999).
  - <sup>36</sup> E. O. Wollan and W. C. Koehler, Phys. Rev. **100**, 545 (1955).
  - <sup>37</sup> E. Dagotto, T. Hotta, and A. Moreo, Physics Reports **344**, 1 (2001).
  - <sup>38</sup> W. Cochran, Adv. in Phys. **9**, 387 (1960).
  - <sup>39</sup> Ph. Ghosez, X. Gonze and J.-P. Michenaud, Europhys. Lett. **33**, 713 (1996).
  - <sup>40</sup> Ph. Ghosez, J.-P. Michenaud and X. Gonze PRB **58**, 6224 (1998).